PCCP

Kinetics of the $HO_2 + NO$ reaction: A temperature and pressure dependence study using chemical ionisation mass spectrometry

Max W. Bardwell,[a] Asan Bacak,[a] M. Teresa Raventos,[a] Carl J. Percival,*[a] Gabriela Sanchez-Reyna[b] and Dudley E. Shallcross[b]

[a] *The School of Science, The Nottingham Trent University, Clifton Lane, Nottingham, UK NG11 8NS. E-mail: carl.percival@ntu.ac.uk*
[b] *Biogeochemistry Research Centre, School of Chemistry, University of Bristol, Cantock's Close, Bristol, UK BS8 1TS*

Received 21st January 2003, Accepted 7th April 2003
First published as an Advance Article on the web 23rd April 2003

The overall rate coefficient (k_2) for the reaction $HO_2 + NO$ (2) has been measured using the turbulent flow technique with chemical ionisation mass spectrometry (CIMS) for the detection of reactants and products. The temperature dependence of the rate coefficient was investigated between 183 and 300 K. Across the temperature range the experimentally determined rate coefficients showed good agreement with previous studies and were fitted using an Arrhenius type analysis to yield the expression $k_2 = (3.98^{+0.29}_{-0.27}) \times 10^{-12}$ exp $[(223 \pm 16.5)/T]$ cm^3 molecules^{-1} s^{-1}. Experiments were carried out in the pressure range of 75 to 220 Torr within the stated temperature range, where the rate coefficients were shown to be invariant with pressure. Such invariance with pressure is in accord with recent theoretical calculations. This work represents an extension to the range of temperature and pressure over which the rate coefficient has been studied. A model of the troposphere has been used to assess the impact of the experimental error of the rate coefficients determined in this study on predicted concentrations of a number of key species, including O_3, OH, HO_2, NO and NO_2. In all cases it is found that the propagated error is rather small and will not in itself be a major cause of uncertainty in modelled concentrations.

Introduction

In the UTLS (upper troposphere lower stratosphere) region catalytic cycles of HO_x (the sum of HO and HO_2) are important in determining the concentration of ozone. In the UT region the fate of the HO_2 radical is influenced by the level of NO_x, *i.e.* the air quality. In the background atmosphere, HO_2 will react with ozone to form OH and O_2 as shown in reaction (1).

$$HO_2 + O_3 \rightarrow OH + 2O_2 \quad (1)$$

OH itself can react with O_3 to reform HO_2 leading to the well-known HO_x cycle that destroys ozone throughout the troposphere and lower stratosphere. However, under elevated levels of NO, HO_2 reacts with NO *via* reaction (2).

$$HO_2 + NO \rightarrow OH + NO_2 \quad (2)$$

$$NO_2 + h\nu(\lambda \leq 410 \text{ nm}) \rightarrow NO + O \quad (3)$$

$$O + O_2 + M \rightarrow O_3 + M \quad (4)$$

The result of reactions (2) to (4) is that ozone is produced. Model simulations by Roelofs and Lelieveld[1] indicated that a substantial amount of ozone in the troposphere is produced *in situ* ($\approx$20%) *via* cycles involving NO_x (Haagen-Smit and Fox[2]). Work by Wennberg *et al.*[3] indicates that measured values of HO_x are often greater than calculated and the presence of larger than expected HO_x values coupled with increases in NO_x from aircraft emissions will lead to significantly higher levels of ozone in the UTLS region. More recent work carried out by Salawitch *et al.*,[4] has shown a discrepancy between calculated and observed levels of HO_x of *ca.* 6% at mid latitudes. In order to be able to successfully model ozone levels it is necessary to know the rate coefficient for reaction (2) over a range of temperatures and pressures pertaining to the UTLS region *i.e. ca.* 180–300 K and 100–250 Torr. Previous studies by Seeley *et al.*,[5] and Howard[6] have established the room temperature rate coefficient for the reaction with relative certainty. Only a limited range of temperatures and pressures have been explored however and Seeley *et al.*,[5] proposed that additional studies of their observed pressure effects would be useful. This work reports on the results of a study carried out on an extended temperature and pressure range with experimental observations compared with recent theoretical calculations.

Experimental

A schematic diagram of the experimental apparatus is shown in Fig. 1. The flow tube was constructed from 22 mm id Pyrex tubing, the walls of which were coated with Halocarbon wax

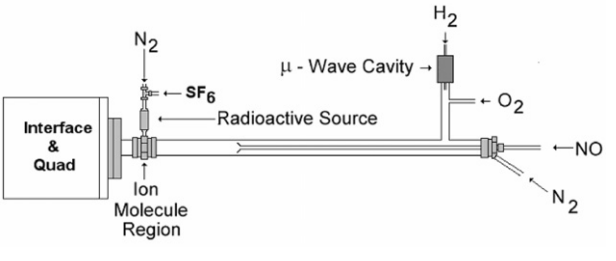

Fig. 1 A schematic diagram of the turbulent flow CIMS instrument.

(Halocarbon Products Inc.). A large flow of nitrogen (ranging from 50 to 130 STP l min^{-1}) was injected upstream of the flow tube. The flow tube was pumped by a rotary pump (Varian, DS1602). Nitrogen oxide was injected through a moveable injector constructed from 4 mm id Pyrex. A propeller shaped Teflon piece (a "turbulizer") designed to enhance turbulent mixing was fixed to the end of the moveable injector. All of the experiments were performed under turbulent flow conditions. Turbulent flow is established when the Reynolds number, *Re*, is greater than 3000. This number is given by:

$$Re = \frac{d\bar{u}\rho}{\mu} \quad \text{(I)}$$

where d is the internal diameter of the flow tube, $\bar{u}$ is the average velocity of the carrier gas, μ is the viscosity of the carrier gas and ρ is the density of the carrier gas.

The ion–molecule region was constructed from 22 mm od Pyrex tubing and a quadrupole mass spectrometer (ABB Extrel Merlin) was located at the end of the ion–molecule region. All gas flows were monitored with calibrated mass flow meters (MKS,1179). The pressures in the flow tube were monitored using a 0–1000 Torr capacitance manometer (MKS, Baratron).

The temperature within the flow tube was maintained within 2 K by placing the flow tube into an insulated chamber that was filled with dry ice. All temperatures were monitored by type K thermocouples. The flow tube temperature was maintained with heating tape (Omega, Heavy duty) regulated by an electronic controller (Carel Universal Infrared control type W) in conjunction with a thermocouple. The flow tube has 5 thermocouples along its length to monitor the temperature of the system. The nitrogen carrier gas was pre-cooled to the same temperature by passing it through a copper coil immersed in liquid nitrogen. The carrier gas temperature was maintained with heating tape (Omega, Heavy duty) regulated by an electronic controller (Carel Universal Infrared control type W) in conjunction with a thermocouple. The temperature profile along the flow tube was checked by placing a thermocouple at the end of the moveable injector, and moving it along the length of the flow tube.

HO_2 was produced upstream of the flow tube *via* the reaction (5)

$$H + O_2 + M \rightarrow HO_2 + M \quad (5)$$

Hydrogen atoms were produced by combining a 2.0 STP l min^{-1} flow of He with a 0.1 to 3 STP cm^3 min^{-1} flow of 1% H_2 in helium, which was then passed through a microwave discharge produced by a Surfatron (Sairem) cavity operating at 165 W. To produce HO_2 radicals, the H atoms were injected into the flow tube *via* a side arm inlet located at the rear of the flow tube and mixed with a 1.0 STP l min^{-1} flow of O_2. At the pressures and flow conditions used in this study, it is calculated that the H atoms have been completely titrated before entering the flow tube. H atoms were periodically titrated with NO_2 to determine the concentration of H atoms produced. In the absence of oxygen, known amounts of NO_2 were added. The mass spectrometer signal (at m/e 46) was monitored with the microwave turned off and then turned on. The decrease in the NO_2 signal observed when the microwave was turned on was attributed to the reaction

$$H + NO_2 \rightarrow NO + OH \quad (6)$$

Using this method it was found that on average 20% of H_2 was dissociated into H atoms. Under normal operating conditions the initial concentration of hydrogen atoms in the flow tube ranged from $(1–10) \times 10^{10}$ molecules cm^{-3}.

NO was introduced into the flow tube *via* the moveable injector by mixing a flow of 10% NO with a 1 STP l min^{-1} flow of nitrogen. In all cases, $[NO] \gg [HO_2]$, so that pseudo-first-order conditions were maintained. Blank runs (with no NO flowing) were carried out to ensure that the HO_2 signal (measured at m/e 140, *i.e.* $SF_4O_2^-$, see later) was not affected by movement of the injector.

NO_2, HO_2 and OH were chemically ionized using SF_6^- as the reagent ion. SF_6^- was generated by combining a 10 STP l min^{-1} flow of N_2 and a 2.5 sccm flow of SF_6 and passing it through a Po(210) Nuclecel ionizer (NRD Inc.). The generated reagent ion was then carried into the ion–molecule region through an injector constructed from 6 mm od stainless steel. A fan shaped turbulizer was attached to the end of the inlet to enhance mixing of the reagent ion with the sampled flow from the flow tube. NO_2 and OH were ionized by SF_6^- *via* electron transfer enabling the species to be detected by their parent ions. HO_2 was detected as $SF_4O_2^-$, presumably through a multi step pathway, as reported by previous studies.[3]

Ions were detected with a quadrupole mass spectrometer in a three-stage differentially pumped vacuum chamber. A sample of the bulk gas flow containing reactant ions is drawn into the front chamber through a 0.6 mm aperture which was held at a potential of −70 V to further focus charged reactant molecules. The front vacuum chamber was pumped by a mechanical pump (Varian DS402) and held at *ca.* 2 Torr. The ions were further focused by a 3 cm od and 0.2 mm id stainless steel plate held at −15 V and passed into a second chamber containing the quadrupole mass filter (ABB Extrel, Merlin). This second chamber was pumped by a turbomolecular pump (Varian V250) backed by a rotary pump (Edwards E2M8). The rear chamber which held the multiplier assembly was pumped by a further turbomolecular pump (Varian V250) backed by a rotary pump (Edwards E2M2). Under typical operating conditions the rear chamber was at a pressure of *ca.* 9×10^{-6} Torr. Ions were detected using a channeltron (Dtech 402A-H) *via* negative ion counting.

Materials

Helium (BOC, CP Grade) was passed through a gas clean oxygen filter (Chrompak) cartridge to remove traces of oxygen, a gas clean moisture filter cartridge (Chrompak) to remove H_2O and a trap held at 77 K containing a molecular sieve (BDH, 4A). NO_2 (98.3%) was purified by repeated freeze–pump–thaw cycles. NO (technical grade) was purified by freeze–pump–thaw cycles, and selective freezing of NO_2 impurities. N_2, O_2 (99.6%) and H_2 (99.999%) were used as supplied.

Results and discussion

Assessment of detector sensitivity

Dilute mixtures of NO_2 were injected *via* the moveable injector into the flow tube with no other gases present and the NO_2^- signal was monitored. From a linear plot of $[NO_2]$ *vs.* NO_2^- signal it is estimated that the sensitivity for NO_2 was 2×10^7 molecule cm^{-3} for a signal to noise ratio of one and a time constant of 1 s. The NO_2 concentrations were corrected to take into account equilibrium concentrations of N_2O_4 in the gas mixtures used. Under the experimental conditions the lifetime of N_2O_4 formed by the equilibrium

$$NO_2 + NO_2 + M \rightleftharpoons N_2O_4 + M \quad (7)$$

is comparable with the time of mixing.[8] This assumption was corroborated by the fact that on the time scale of the experiment no change in $[NO_2]$ was observed.

Calibration of the HO_2 signal was achieved by adding a large excess of NO *via* the moveable injector at a constant contact time and by monitoring the resultant NO_2 formed by

reaction with HO_2

$$HO_2 + NO \rightarrow NO_2 + OH \quad (2)$$

Sufficient NO was added to ensure complete removal of HO_2, confirmed by a constant NO_2^- signal with increasing [NO]. It is assumed that $[NO_2]_{observed} = [HO_2]$. This procedure was repeated for several different hydrogen atom concentrations and yielded a linear plot of $SF_4O_2^-$ signal *vs.* $[NO_2]_{observed}$. It is estimated that the sensitivity for HO_2 was 1×10^7 molecule cm^{-3} for a signal to noise ratio of one and a time constant of 1 s.

Calibration of the OH sensitivity was performed in a manner described by Canosa-Mas and Wayne.[9] OH radicals were produced *via* the reaction

$$H + NO_2 \rightarrow OH + NO \quad (6)$$

H-atoms were injected into the flow tube *via* a side arm inlet located at the rear of the flow tube and in the absence of oxygen, known amounts of NO_2 were added *via* the moveable injector. The mass spectrometer OH^- signal (at m/e 17) was monitored as a function of the NO_2 concentration added at various contact times. It is estimated that the sensitivity for OH was 4×10^7 molecule cm^{-3} for a signal to noise ratio of one and a time constant of 1 s.

Rate coefficient determination

The rate coefficient for reaction (2) was measured by monitoring HO_2 concentration profiles at $m/e = 140$ under pseudo-first-order conditions with $[HO_2] = (1-10) \times 10^{10}$ molecule cm^{-3} and $[NO] = (1-12) \times 10^{12}$ molecule cm^{-3}. First order decay rates (k_{1st}) were obtained by a linear regression of the plots of ln (HO_2 signal) *vs.* contact time (as shown in Fig. 2). Each of these plots was essentially linear for all the experiments indicating the absence of any secondary chemistry effects. This process was repeated for at least ten different values of [NO] at each pressure studied. The values of k_{1st} were then plotted *vs.* [NO] as shown in Fig. 3. These data points were fitted with a linear least squares routine, the slope of which provided the effective bimolecular rate constant, k_2. Table 1 lists the bimolecular rate coefficients obtained in this study. This approach for the determination of the effective bimolecular rate coefficient assumes that deviations from the plug flow approximation are negligible. Under the experimental conditions used, Seeley *et al.*,[10] estimated that deviations from the plug flow approximation result in apparent rate coefficients that are at most 8% below the actual values. Hence, flow corrections were neglected, as they are smaller than the sum of other systematic experimental errors.

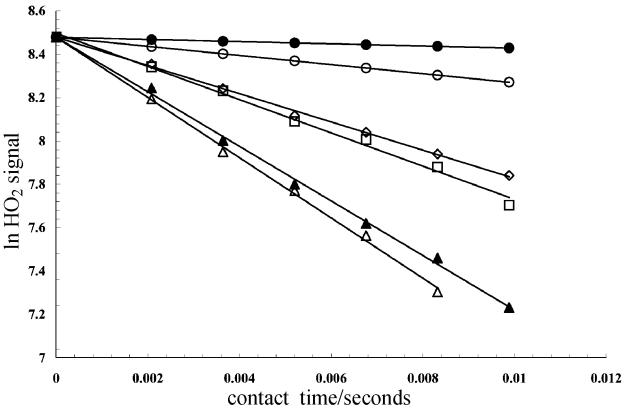

Fig. 2 A typical set of psuedo-first-order plots. For [NO] of ● 9.28×10^{11} molecules cm^{-3}; ○ 2.29×10^{12} molecules cm^{-3}; ◇ 6.88×10^{12} molecules cm^{-3}; □ 9.05×10^{12} molecules cm^{-3}; ▲1.38×10^{13} molecules cm^{-3} and Δ 1.85×10^{13} molecules cm^{-3}.

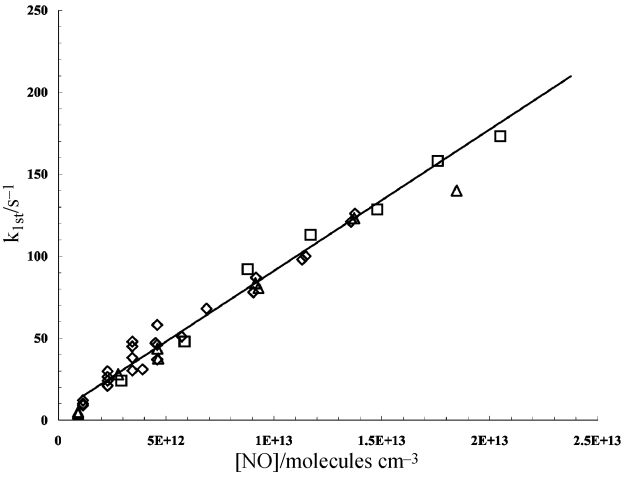

Fig. 3 Second order plot showing the results of experiments at three different pressures at 300 K. ◇ 75 Torr data, □ 100 Torr data and Δ 200 Torr data. The line is the linear least squares fit.

The data shown in Fig. 3 are for experiments carried out at three different pressures at 298 K. Within error each data set produces the same effective bimolecular rate coefficient indicating that the rate coefficient is invariant with pressure. If all the data are combined an effective bimolecular rate coefficient at 298 K of $(8.43 \pm 0.20) \times 10^{-12}$ cm^3 $molecule^{-1}$ s^{-1} which is in agreement with previous studies.[5,7,11–18]

The rate coefficient for reaction (2) was also studied over the temperature range 183–300 K. Table 1 summarises the effective bimolecular rate coefficients obtained in this study. The rate coefficients increased by *ca.* 65% as the temperature was lowered from 300 to 183 K. The rate coefficients were determined as a function of pressure from 75–200 Torr, and no effect of pressure on the measured rate coefficients was observed over the temperature range studied. From the data in Table 1 it is possible to carry out an Arrhenius type analysis of the temperature dependence yielding an "Arrhenius" expression of $k(T) = (3.98^{+029}_{-027}) \times 10^{-12} \exp[(223 \pm 16.5)/T]$ cm^3 $molecule^{-1}$ s^{-1}; the uncertainty is given at the one standard deviation level, *i.e.* an apparent negative activation energy is observed. Two other thorough studies have been carried out of the temperature dependence of reaction (2) below 300 K, a high pressure flow tube study by Seeley *et al.*,[5] and a low pressure flow tube study by Howard.[6] A comparison of data from this study with previous low temperature studies by Howard and Seeley *et al.*,[5] is shown in Fig. 4. The graph shows close agreement between the results of all three studies and this indicates no significant pressure dependence for the rate coefficient for reaction (2) in the 183–300 K range. If all the data is combined an average "Arrhenius" expression is calculated to be $(3.26^{+029}_{-026}) \times 10^{-12} \exp[(275 \pm 21)/T]$ cm^{-3} $molecules^{-1}$ s^{-1}.

Table 1 Experimentally determined rate constants for reaction (2) from studies at $T < 300$ K

Temperature/K	Pressure/Torr	Rate coefficient/ 10^{-12} cm^3 $molecule^{-1}$ s^{-1}
298	75	8.62
298	100	8.57
298	200	8.09
253	100	9.53
253	200	9.68
223	100	10.4
213	200	12.0
193	100	12.8
193	200	12.3

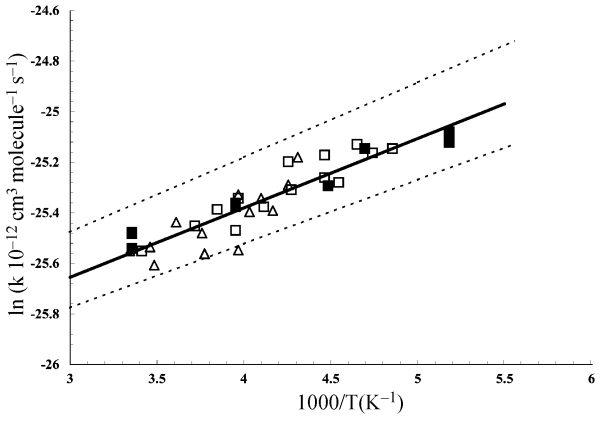

Fig. 4 Arrhenius plot for the $HO_2 + NO$ reaction combining the data from this work and those of the two previous studies below 300 K. The solid line is the average of all the data points. The dashed line is equivalent to one standard deviation. ■ Data from this work, □ data from Seeley *et al.*, and Δ data from Howard.

Mechanism

The negative temperature dependence of the rate coefficient for reaction (2) suggests that it proceeds through the formation of an $[HO_2NO]^*$ intermediate. The intermediate could then re-dissociate back to reactants, undergo bond fission to yield products or undergo collisional stabilisation. The elements of the mechanism may be summarised as:

$$HO_2 + NO \rightarrow [HO_2NO]^* \quad (8)$$

$$[HO_2NO]^* \rightarrow HO_2 + NO \quad (-8)$$

$$[HO_2NO]^* \rightarrow OH + NO_2 \quad (9)$$

$$[HO_2NO]^* + M \rightarrow HO_2NO + M \quad (10)$$

The absence of any experimentally observed pressure dependence, and the excellent agreement with the low pressure rate coefficients reported by Howard,[6] suggests that the $[HO_2NO]^*$ intermediate is too short lived to be affected by collisions with the bulk N_2 gas even at the extended temperatures and pressures of this study.

To further elucidate the fate of any intermediates formed the products of reaction (2) were also monitored. Fig. 5 shows a typical plot of HO_2, NO_2 and OH signal as a function of contact time. The curve passing through the HO_2 is the experimentally determined loss rate of reactants, and NO_2 assumes 100% formation of NO_2 and thus a first order appearance of reactants. Fig. 5 shows that the OH signal decays as a function of contact time as a consequence of the secondary reaction with NO:

$$OH + NO + M \rightarrow HONO + M \quad (11)$$

The curve passing through the OH signal is based on the combination of the rate of production of OH from reaction (2) and the rate loss of OH from reaction (11). Over the temperature and pressure range studied there was no evidence, within experimental error, for the formation of any stabilised adducts or secondary product channels, *i.e.* it can be assumed that the reaction proceeds $100 \pm 5\%$ *via* the formation of OH and NO_2.

Chakraborty *et al.*,[19] have recently carried out an extensive theoretical study of the reaction between OH and NO_2 and considered both the channel forming $HONO_2$ and HO_2NO. These workers have also explored reaction (2) in detail as a result of their study and compared RRKM predictions with available kinetic data at that time. It is clear from the work of Chakraborty *et al.*,[19] that the HO_2NO would not be stabilised at the pressures studied in this work. Simple calculations based on QRRK theory[20,21] using the thermodynamic data from Chakraborty *et al.*,[19] indeed confirm that several atmospheres pressure would be required to stabilise the adduct. These calculations show that once the energised adduct is formed, it almost exclusively decomposes *via* simple bond fission to yield OH and NO_2. Re-dissociation and stabilisation of the intermediate are all inefficient processes in comparison. Several points should be noted. First, the product channel to form OH and NO_2 should dominate on thermodynamic grounds since the reaction is exothermic. Second, the calculations suggest that the rate determining step for reaction (2) is actually reaction (8), *i.e.* how quickly the HO_2NO intermediate formed. Third, as the re-dissociation reaction is negligible at all pressures over the temperature range studied, the rate coefficient cannot be pressure dependent for reaction (2) which is in good agreement with the experimentally observed rate coefficients of both this work and that of Seeley *et al.*.[5] Fourth, the rate coefficient for reaction (2) might be expected to decrease with increasing temperature, because the re-dissociation of the HO_2NO could begin to compete with channel (9) which is in agreement with the experimentally observed apparent "negative" activation energy. Finally, these calculations suggest that the HO_2NO intermediate would not be stabilised, even at extremely high pressures; which is in agreement with the product studies carried out in this work, *i.e.* no evidence for the formation of any products other than OH and NO_2.

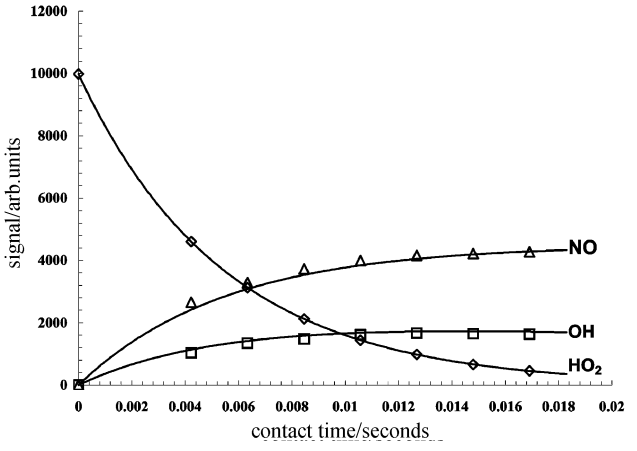

Fig. 5 Signal intensity as a function of injector position. □ OH, Δ NO_2, ◇ HO_2. The curves fitted to the NO_2 and HO_2 data are calculated for a first order appearance and decay of products and reactants, respectively.

Atmospheric implications

The importance of reaction (2) for the *in vivo* production of ozone in the troposphere is well known.[1] It is therefore extremely important to characterise the rate coefficients for such reactions over a wide range of pressure and temperature. Field *et al.*,[22] and many others have noted the importance of reaction (2) in an autocatalytic production of HO_x, *i.e.*

$$CO + OH + O_2 \rightarrow HO_2 + CO_2 \quad (12)$$

$$HO_2 + NO \rightarrow OH + NO_2 \quad (2)$$

$$NO_2 + h\nu \rightarrow NO + O \quad (3)$$

$$O + O_2 + M \rightarrow O_3 + M \quad (4)$$

$$O_3 + h\nu \rightarrow O_2 + O(^1D) \quad (13)$$

$$O(^1D) + H_2O \rightarrow OH + OH \quad (14)$$

Net: $CO + 2h\nu + H_2O + O_2 \rightarrow 2OH + CO_2$

Therefore model sensitivity studies have been performed, using CiTTy CAT, a tropospheric trajectory model.[23] The model was run for a variety of scenarios, replicating those conditions prescribed in the Photochemistry-intercomparison exercise.[24] Details of the initial conditions and model scenarios used can be found in the summary paper by Olson *et al.*[24] Essentially, the model was run under three surface scenarios, clean marine, background continental and urban conditions, and two scenarios away from the surface, a polluted plume at 4 km and a clean air scenario at 8 km. These five scenarios were originally chosen for the intercomparison to cover the range NO_x/VOC encountered in the troposphere and its influence on ozone production and destruction. The CiTTy CAT model contains a detailed chemistry scheme with 13 non-methane hydrocarbons and for each scenario the model was integrated forward in box model mode for five days. Three integrations were performed for each of the five atmospheric conditions described, a base case where the central Arrhenius parameters were used, a 'high' k_2 case, where the largest A factor and lowest Ea, within measurement error in this study were used and a 'low' k_2 case, where the smallest A factor and highest Ea, within measurement error in this study were used. Comparisons between each set of three integrations were then made for a range of species, and those with the most significant impact being O_3, OH, HO_2, NO and NO_2. In all cases, within the experimental error of this study, model O_3 did not deviate by more than 1%. At low model NO_x (less than a few ppb) OH varies by 2% (increasing with high k_2) and at 5 ppb NO_x, the variation in OH has risen to just over 4% at all altitudes. HO_2 is slightly more sensitive to k_2, as one would expect, decreasing in concentration in the model with a rise in k_2. At the surface HO_2 varies from 1–5% as NO_x increases up to *ca.* 5 ppb, however, at 8 km, at the very highest NO_x (5 ppb), HO_2 varies by as much as 12%. NO itself varies (decreasing with a higher k_2) from 3–6% at the surface and up to 12% at 8 km, whilst NO_2 varies by 7% at most at all altitudes. It is concluded that the impact of the experimental error in the measurement of k_2 in this study has an insignificant effect on modelled species concentrations in the troposphere, although it is noted that at high NO_x levels, both HO_2 and NO vary by more than 10% when using the extreme values of k_2. The discrepancy between model and measured HO_x in the UT cannot be explained by experimental errors in k_2.

Conclusions

Our data indicates that reaction (2) has a significant negative temperature dependence, as suggested by previous studies of the reaction.[5,6] The results presented in this article represent an extension in the range of temperatures over which reaction (2) has been studied experimentally. Our results are in excellent agreement with extrapolations to 183 K based on previous higher temperature measurements extrapolated to 183 K. The negative temperature dependence of the rate coefficient for reaction (2) suggests that it proceeds through the formation of an energised intermediate (HO_2NO^*). Over the temperature range studied the rate coefficient for reaction (2) was found to be invariant with pressure. In conjunction with product studies and theoretical calculations, our results suggest that the HO_2NO^* intermediate is too short lived to be affected by collisions and it exclusively decomposes *via* simple bond fission to yield OH and NO_2. Atmospheric model sensitivity studies, using a tropospheric trajectory model, were performed to assess the impact of the experimental errors of reaction (2) on tropospheric O_3 production. It was found that within the experimental error of the studies, model O_3 did not deviate by more than 1%. The model sensitivity study suggests that the uncertainty associated with the rate parameters for reaction (2) will have only a minor impact on the evolution of chemical species in atmospheric models.

Acknowledgements

The authors gratefully acknowledge the financial support of NERC research grant reference number NER/T/S/1999/00111. MB thanks NERC for a studentship and GS-R thanks the Instituto Mexicano del Petróleo for a studentship. The Biogeochemistry research centre at Bristol is a joint initiative between the School of Chemistry and the Departments of Geography and Geology.

References

1 G. J. Roelofs and J. Lelieveld, *Tellus*, 1997, **49B**, 38–55.
2 A. J. Haagen-Smit and M. M. Fox, *Ind. Eng. Chem.*, 1956, **48**, 1484.
3 P. O. Wennberg, T. F. Hanisco, L. Jaegle, D. J. Jacob, E. J. Hintsa, E. J. Lazendorf, J. G. Anderson, R.-S. Gao, E. R. Keim, S. G. Donnelly, L. A. Del Negro, D. W. Fahey, S. A. Mckeen, R. J. Salawitch, C. R. Webster, R. D. May, R. L. Herman, M. H. Proffitt, J. J. Margitan, E. L. Atlas, S. M. Schauffler, F. Locke, C. T. McElroy and T. P. Bui, *Science (Washington, D. C.)*, 1998, **279**, 49–53.
4 R. J. Salawitch, P. O. Wennberg, G. C. Toon, B. Sen and J.-F. Blavier, *Geophys. Res. Lett.*, 2002, **29**, 1–4.
5 J. V. Seeley, R. F. Meads, M. J. Elrod and M. J. Molina, *J. Phys. Chem.*, 1996, **100**, 4026–4031.
6 C. J. Howard, *J. Chem. Phys.*, 1979, **71**, 2352–2359.
7 M. J. Elrod, R. F. Meads, J. B. Lipson, J. V. Seeley and M. J. Molina, *J. Phys. Chem.*, 1996, **100**, 5808–5812.
8 P. Borrell, C. J. Cobos and K. Luther, *J. Phys. Chem.*, 1988, **92**, 4377–4384.
9 C. E. Canosa-Mas and R. P. Wayne, *Int. J. Chem. Kinet.*, 1990, **22**, 829–841.
10 J. V. Seeley, J. T. Jayne and M. J. Molina, *Int. J. Chem. Kinet.*, 1993, **25**, 571–594.
11 J. J. Martigan and J. G. Anderson, results presented at the *13th Informal Conference on Photochemistry*, Clearwater Beach, FL, 1978.
12 F. Kaufman and B. Reimann, Results presented at *13th Informal Conference on Photochemistry*, Clearwater Beach, FL, 1978.
13 C. J. Howard and K. M. Evenson, *Geophys. Res. Lett.*, 1977, **4**, 437–440.
14 M. T. Leu, *J. Chem. Phys.*, 1979, **70**, 1662–1666.
15 I. Glaschick-Schimpf, A. Leiss, P. B. Monkhouse, U. Schurath, K. H. Becker and E. H. Fink, *Chem. Phys. Lett.*, 1979, **70**, 318–323.
16 W. Hack, W. Preuss, F. Temps and H. G. G. Wagner, *Int. J. Chem. Kinet.*, 1980, **12**, 851–860.
17 B. A. Thrush and J. P. T. Wilkinson, *Chem. Phys. Lett.*, 1981, **84**, 17–19.
18 A. A. Jemi-Alade and B. A. Thrush, *J. Chem. Soc., Faraday Trans.*, 1990, **86**, 3355–3363.
19 D. Chakraborty, J. Park and M. C. Lin, *J. Chem. Phys.*, 1998, **231**, 39–49.
20 L. S. Kassel, *J. Phys. Chem.*, 1928, **32**, 1065.
21 A. M. Dean, *J. Phys. Chem.*, 1985, **89**, 4600–4608.
22 R. J. Field, P. G. Hess, L. V. Kalachev and S. Madronich, *J. Geophys. Res.*, 2001, **106**, 7553–7565.
23 M. J. Evans, D. E. Shallcross, K. S. Law, J. O. F. Wild, P. G. Simmonds, T. G. Spain, P. Berrisford, J. V. Methven, A. C. Lewis, J. B. McQuaid, M. J. Pilling, B. J. Bandy, S. A. Penkett and J. A. Pyle, *Atmos. Environ.*, 2000, **34**, 3843–3863.
24 J. Olson, M. Prather, T. Bernsten, G. Carmichael, R. Chatfield, P. Connell, R. Derwent, L. Horrowitz, S. Jin, M. Kanakidou, P. Kasibhatla, R. Kotamarthi, M. Kuhn, K. Law, J. Penner, L. Perliski, S. Sillman, F. Stordal, A. Thompson and O. Wild, *J. Geophys. Res.*, 1997, **102**, 5979–5991.